Article

Photocatalytic Oxidization Based on TiO2/Au Nanocomposite Film for Total-Phosphorus (TP) Pretreatment

Jiajie Wang , Seung Deok Kim , Jae Yong Lee , June Soo Kim , Noah Jang , Hyunjun Kim , Da Ye Kim , Yujin Nam , Maeum Han , Seong Ho Kong *

Posted Date: 23 January 2024

doi: 10.20944/preprints202401.1637.v1

Keywords: total phosphorus; pretreatment; photocatalyst; lab-on-a-chip, TiO2/Au nanocomposite film

Article

Photocatalytic Oxidization Based on TiO_2/Au Nanocomposite Film for Total-Phosphorus (TP) Pretreatment

Jiajie Wang †, Seung Deok Kim †, Jae Yong Lee, June Soo Kim, Noah Jang, Hyunjun Kim, Da Ye Kim, Yujin Nam, Maeum Han and Seong Ho Kong *

School of Electronic and Electrical Engineering, Kyungpook National University, Daegu 41566, Korea

* Correspondence: shkong@knu.ac.kr (S.H.K); Tel.: +82-(0)53-940-8679 (S.H.K)

† Authors contributed equally to this work.

Abstract: Phosphorus, an essential rare element in aquatic ecosystems, plays a key role in maintaining ecosystem balance. However, an excess of phosphorus will lead to eutrophication and algal proliferation. To prevent eutrophication, it is crucial to pretreat and measure the concentration of total phosphorus (TP). Compared with conventional TP pretreatment equipment (autoclave), a lab-on-a-chip detection device fabricated through micro-electromechanical system technology using titania (TiO_2) as a photocatalyst is more convenient, efficient, and cost-effective. However, the wide bandgap of TiO_2 (3.2 eV) limits the photocatalytic activity. To address this problem, this paper describes the preparation of a TiO_2/Au nanocomposite film by electron-beam evaporation and atomic layer deposition, based on the introduction of a gold film and TiO_2 on a quartz substrate. The photocatalytic degradation properties of TiO_2/Au nanocomposite films with thicknesses of 1, 2, 3, and 4 nm are assessed using rhodamine B as a pollutant. Experimental results demonstrate that the deposition of a gold film with different thicknesses can enhance the photocatalytic degradation efficiency through synergetic reactions in the charge separation process on the surface. The optimal photocatalytic efficiency is achieved when the deposition thickness is 2 nm, and it decreases with further increase in the thickness. When the photocatalytic reaction time is 15 min, the LOC device with a 2-nm-thick gold layer and autoclave exhibit similar TP pretreatment performance. Therefore, the proposed LOC device based on photocatalysis technology can address the limitation of conventional autoclave equipment, such as large volume, long processing time, and high cost, thereby satisfying the growing demand for on-site evaluation.

Keywords: total phosphorus; pretreatment; photocatalyst; lab-on-a-chip; TiO_2/Au nanocomposite film

1. Introduction

With progress in human industrialization and urbanization, although human living standards have continually improved, challenges such as environmental pollution, resource depletion, and ecosystem destruction have emerged. Phosphorus, a crucial trace element in plant photosynthesis, plays a vital role in maintaining ecological balance [1]. However, the accelerated pace of human industrialization has disrupted the balance of trace elements in the ecosystem. In particular, the discharge of phosphorus-containing substances into rivers and lakes has led to frequent occurrences of algal blooms and water eutrophication [2–5].

Given these concerns, it becomes essential to monitor the concentration of total phosphorus (TP) in aquatic ecosystems to prevent eutrophication. As phosphorus typically exists in nature in compound forms, it is challenging to directly detect the TP concentration from compounds containing phosphorus. This necessitates the conversion of organic and inorganic compounds containing phosphorus into easily detectable phosphate (PO_4^{3-}) through pretreatments in advance, a process known as TP pretreatment. Compared with the conventional mode of using autoclaves for

pretreatment, photocatalysis technology has emerged as a promising solution to address the abovementioned challenges. Through photocatalytic reactions using potassium persulfate ($K_2S_2O_8$) as the oxidizing agent, organic and inorganic compounds containing phosphorus can be pretreated into easily detectable PO_4^{3-}, and the phosphorus content in water can be monitored through the change in the PO_4^{3-}concentration. Because the PO_4^{3-} obtained after pretreatment is pure white, it is stained using a coloring agent, exhibiting various shades of blue based in the PO_4^{3-} concentration. Finally, ultraviolet–visible (UV–vis) spectrophotometry is applied to test the absorbance of the colored sample.

Titanium dioxide (TiO_2), an important semiconductor material with applications in various fields—such as photocatalytic water splitting for hydrogen production, sensors, solar cells, self-cleaning coating, degradation of organic pollutants, and TP or total nitrogen photocatalyst—has attracted substantial research attention owing to its non-toxic, strong oxidation properties, earth abundance, and stable chemical structure [6–8]. However, the wide bandgap (3.2 eV) of TiO_2 limits the separation and transport efficiency of its photogenerated carriers. Moreover, the rapid recombination of photogenerated carriers restricts the photocatalytic activity of TiO_2.

Considering these aspects, it becomes necessary to identify techniques to improve the photocatalytic performance of TiO_2. At present, doping with noble metals (e.g., Au, Ag, and Pt) is the prevalent method to improve the photocatalytic performance of TiO_2 [9]. Therefore, in this work, TiO_2/Au nanocomposite film test devices with different gold film thicknesses were prepared through various methods, such as electron beam (e-beam) evaporation and atomic layer deposition (ALD). The photocatalytic activity of TiO_2 was enhanced through the synergistic action of TiO_2 and gold nanoparticles [10]. The degradation properties of TiO_2/Au nanocomposite film under different photocatalytic reaction durations were evaluated using rhodamine B (RhB) as a pollutant in microfluidic channels composed of polydimethylsiloxane (PDMS). Results demonstrated that the TiO_2/Au nanocomposite film exhibited the highest photocatalytic activity when the gold film deposition thickness was 2 nm. With further increase in the deposition thickness of the gold film, the photocatalytic efficiency decreased, attributable to a reduction in the direct contact surface area between gold particles and TiO_2, which lowered the reaction rate. Additionally, multilayer stacking reduced the light absorption and utilization. Although noble metal deposition can enhance the photocatalytic performance of TiO_2, it is necessary to consider the influence of its preparation method, film deposition thickness, crystal structure, and size and shape of noble metal particles on the photocatalytic degradation performance of TiO_2 [11].

Finally, analytes with the same TP concentration were selected and pretreated using conventional equipment (an autoclave) and the proposed TiO_2/Au nanocomposite film detection device with a gold film deposition thickness of 2 nm. The photocatalytic reaction time of the TiO_2/Au nanocomposite film was varied by adjusting the micropump flowrate. The absorbance peak values under different photocatalytic reaction durations were compared with those obtained using the autoclave pretreatment method. The results demonstrated that the lab-on-a-chip (LOC) device with a photocatalytic reaction time of up to 15 min could achieve a pretreatment performance comparable with that attained using the autoclave. To assess the feasibility and accuracy of the experimental results, compounds with different phosphorus concentrations were subjected to pretreatment through a 15-min photocatalytic reaction, and the findings were compared with data corresponding to the autoclave. The experimental results demonstrated that the LOC device with a gold film deposition thickness of 2 nm can effectively replace the traditional autoclave device when the photocatalysis duration is 15 min.

2. Materials and Methods

2.1. TP Analysis

The commonly used methods for detecting the TP concentration can be divided into two categories [12]. Both types of methods include pretreatment and measurement of TP samples, differing mainly in terms of the TP pretreatment strategy. The first type of approach uses a

 doi:10.20944/preprints202401.1637.v1

conventional autoclave to pretreat the organic and inorganic compounds containing phosphorus into easily detectable PO_4^{3-} under high temperature (121 °C) and high pressure (1.1 kg/cm^2), adopting $K_2S_2O_8$ as the oxidizing agent. This conventional TP pretreatment method requires at least 30 min of oxidation of the sample under harsh experimental conditions (high temperature and high pressure). Moreover, following the reaction, additional time is required for cooling treatment to facilitate subsequent sample analysis.

The alternative TP pretreatment method involves a portable and inexpensive LOC device prepared using micro-electro-mechanical system technology [13,14]. Using the principle of photocatalysis, a $K_2S_2O_8$ oxidizing agent is used to pretreat phosphorus-containing compounds into PO_4^{3-} under UV (365 nm) light irradiation. Owing to its high photocatalytic activity, TiO_2 is widely used in the field of photocatalysis. Therefore, in this study, TiO_2 in the solid film form is selected as the photocatalyst to ensure the efficiency and controllability in experiments.

After pretreatment, a mixture (colorant) containing ammonium molybdate $(NH_4)_6Mo_7O_{24}{\cdot}4H_2O$) and ascorbic acid ($C_6H_8O_6$) is added to stain the samples. As the PO_4^{3-} concentration increases, the color of the dyed sample transitions from light blue to dark blue. The phosphorus compounds and oxidizing agent are introduced into the LOC test device via a micropump. The photocatalytic reaction time is controlled by adjusting the flow rate of the micropump. Finally, the absorbance of samples subjected to different photocatalytic reaction durations are measured through UV–vis spectrophotometry. The process flows of the two types of TP pretreatment and measurement methods are shown in Figure 1.

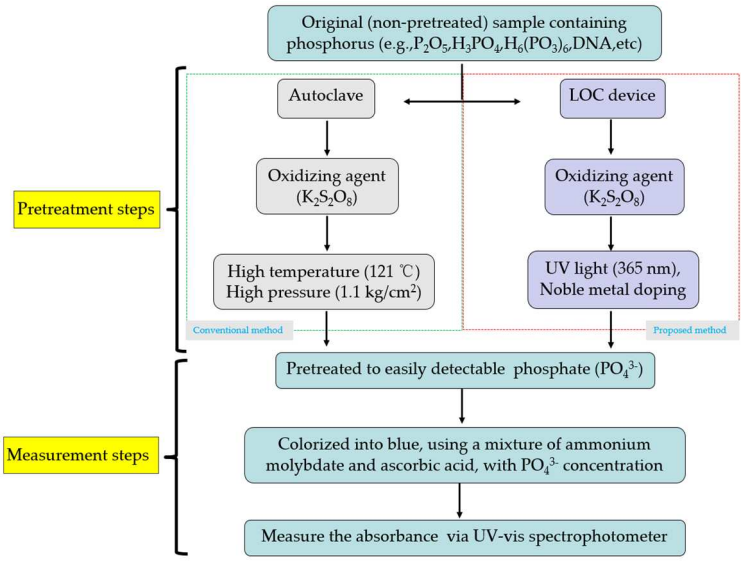

Figure 1. Process flow of total-phosphorus (TP) analysis using an autoclave and a LOC device.

2.2. Principle of Photocatalysis

Since the discovery of the Honda–Fujishima effect in 1967, the field of photocatalysis has garnered significant research attention and witnessed considerable progress in recent decades. Photocatalysis technology is based on the absorption and utilization of light by a catalyst to produce a new active oxide for participating in chemical reactions.

The principle of the photocatalytic reaction of TiO_2 [15] can be explained as follows: When incident light with photon energy greater than the bandgap width of TiO_2 irradiates the sample surface, the negatively charged valence electrons (e^-) in TiO_2 transition from the valence band to the conduction band due to excitation, leaving positively charged holes (h^+) and leading to the formation of electron–hole pairs. Under the action of the space electric field, the electron–hole pairs relocate to different positions on the TiO_2 surface, and redox reactions occur with the substances on the surface. Electrons combine with oxygen molecules dissolved in water to produce superoxide ion free radicals ($\bullet O_2^-$), while holes convert water molecules or hydroxide ions adsorbed on the TiO_2 surface into hydroxyl radicals ($\bullet$OH). Superoxide ions and hydroxyl radicals are highly oxidizing and can

 doi:10.20944/preprints202401.1637.v1

decompose organic compounds in water into inorganic compounds such as carbon dioxide (CO_2) and water (H_2O) [16,17]. The chemical equations representing the roles of the electron–hole pairs are presented below.

$$TiO_2 + h\nu \Rightarrow \text{Electrons } (e^-) + \text{Holes } (h^+) \quad (1)$$

$$\text{Electrons } (e^-) + O_2 \Rightarrow \bullet O_2^- \quad (2)$$

$$\text{Holes } (H^+) + H_2O \Rightarrow H^+ + \bullet OH \quad (3)$$

$$\text{Holes } (H^+) + OH^- \Rightarrow \bullet OH \quad (4)$$

These equations indicate that the main agents driving photocatalytic degradation are superoxide ions, hydroxyl radicals, and other intermediates, The number of such intermediates is controlled by the number of electron–hole pairs generated by UV irradiation. Therefore, the key to improving the photocatalytic efficiency of TiO_2 is to increase the concentration of photogenerated carriers. Many researchers have proposed strategies to enhance the photocatalytic performance of TiO_2, including improving the crystal structure, inhibiting electron–pair recombination, modifying the material surface, metal doping, and using graphene or other novel materials. In this study, the photocatalytic activity of TiO_2 is improved through gold-film doping. The synergistic reaction of doped TiO_2 and gold nanoparticles is shown in Figure 2. In the TiO_2/Au nanocomposite film, electrons migrating to valence bands flow from TiO_2 to gold nanoparticles due to the energy band difference between them, thereby increasing the carrier concentration and impeding their recombination. In addition, gold nanoparticles and possible defect sites at the interface of TiO_2 promote electron migration.

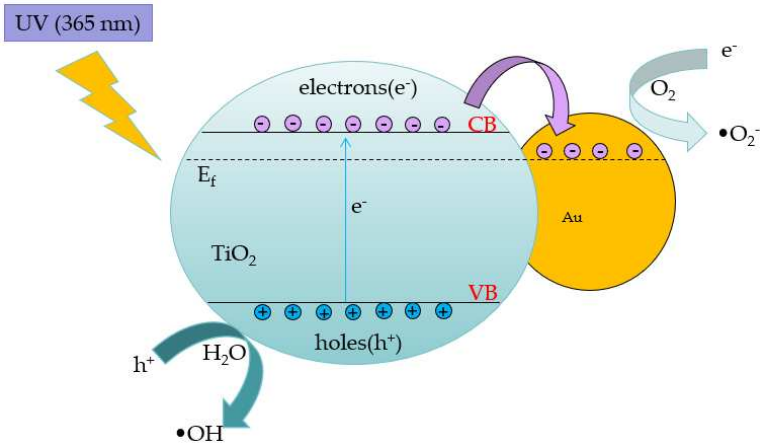

Figure 2. Schematic of pollutant degradation mechanism by TiO_2/Au nanocomposite film under UV irradiation.

2.3. Design and Fabrication of LOC Test Device

Figure 3a shows a top view of the pre-designed microchannel for TP pretreatment, including a mixing channel and pretreatment channel. The length and width of the microchannel, excluding the input–output ports for connecting hoses, are 37 mm and 31 mm, respectively. The width and height of the mixing and pretreatment channels are 1 mm and 0.1 mm, respectively. To ensure thorough mixing of the oxidant and analyte, square obstacles with a width of 0.3 mm are placed within the mixing channel [13]. Two input ports in the mixing channel section facilitate the entry of the analyte and oxidant ($K_2S_2O_8$), and an output port at the end of the pretreatment channel enables the collection of the liquid after the photocatalytic reaction.

Figure 3b presents a schematic of the photocatalytic reaction occurring within the microchannel. The analyte fed to the input port gradually flows toward the output under the action of the micropump. When UV light with a wavelength of 365 nm irradiates the TiO_2/Au nanocomposite film, the separated electrons react with oxygen molecules to produce superoxide ions ($\bullet O_2^-$), while the holes react with water molecules to form hydroxyl radicals (•OH). Superoxide ions and hydroxyl radicals, as critical intermediates in photocatalytic reactions, significantly affect the photocatalytic efficiency [18,19].

 doi:10.20944/preprints202401.1637.v1

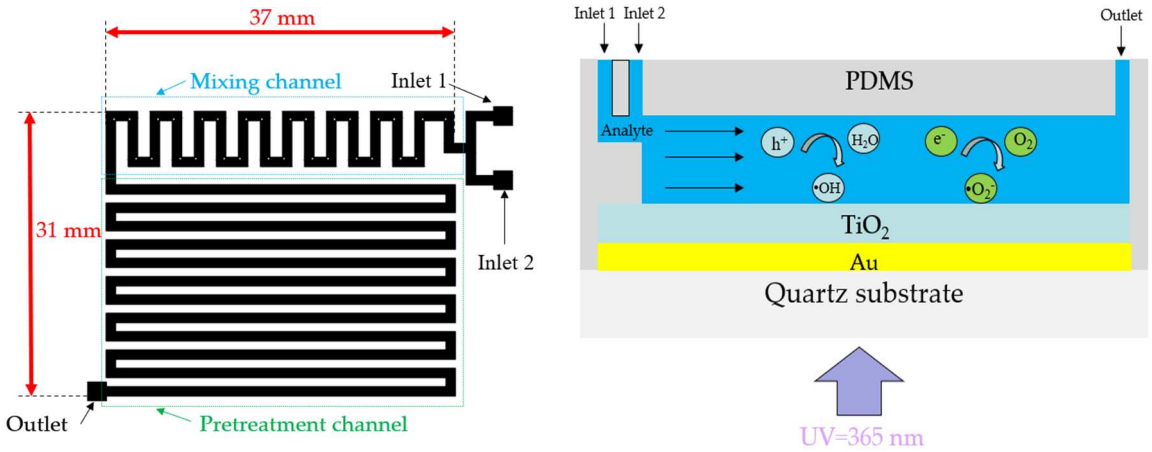

(**a**) (**b**)

Figure 3. (a) Top view of the pre-designed microchannel of LOC device and **(b)** schematic of the photocatalytic microfluidic reactor.

Before preparing the microchannel, a PDMS mold is developed using a 6-in Si substrate through the photolithography process. [12]. The fabrication processes of the PDMS mold and PDMS are illustrated in Figure 4a. First, SU-8 2075 negative photoresist (PR) is used to prepare a PR coating on the Si substrate through the spin-coating method. Subsequently, the PR coating is soft baked at different temperatures for different durations. Next, the baked PR is exposed to a pre-designed photomask plate and subjected to post-exposure baking at different temperatures for different durations. Finally, the SU-8 developer is used to develop the baked PR for 10 min (or more) to remove the PR outside the exposure area, forming a microfluidic channel mold.

After obtaining the PDMS mold, it is wrapped with tinfoil, and a mixture of 44 g PDMS polymer base and curing agent (mixing ratio: 10 to 1) is poured into the mold. A 20-min vacuum treatment is implemented to remove the bubbles in the mixture. Next, the PDMS solution is baked at 70 °C for 2 h to transform the liquid into a transparent solid. The transparent solid PDMS layer is peeled off and catted to obtain a pattern inverse to that of the PDMS mold. The height and width of the microchannel are 0.1 mm and 1 mm, respectively. Inlet and outlet holes are punched in pre-designed locations.

The process of fabricating the TiO_2/Au nanocomposite film is illustrated in Figure 4c. The pre-deposited 6-in quartz substrate is cleaned using acetone, isopropyl alcohol, and deionized water. Subsequently, the dried, contamination-free quartz substrate is placed in the e-beam evaporation chamber (SORONA SRN-200, Gyeonggi-do, Korea), and gold films with thicknesses of 1, 2, 3, and 4 nm are deposited. The deposited gold films are placed in a heating furnace for high-temperature annealing (600 °C, 1 h). This process transforms the shape of the deposited gold particles from island-like to nearly spherical, thereby increasing the average interparticle distance [8]. In the next step, TiO_2 films with a thickness of 15 nm are deposited onto the surface of gold nanoparticles using ALD equipment (CN1 Atomic Classic, Gyeonggi-do, Korea), employing alternating pulses of tetrakisdimethylamido titanium (TDMATi) and H_2O as precursors in an Ar atmosphere [20,21]. When the deposition temperature is 150 ℃, the thickness of TiO_2 deposited per cycle is approximately 0.57 Å, and 270 deposition cycles generate TiO_2 films with a thickness of 15 nm. For comparison, pure TiO_2 films with a thickness of 15 nm are also deposited on a quartz substrate using the same method. Finally, the deposited TiO_2 film is annealed at 500 ℃ for 1 h to transform its crystal structure into the anatase phase, characterized by high photocatalytic performance [22–24].

After prefabricating the TiO_2/Au nanocomposite film and PDMS, a thin mixed liquid coating of PDMS polymer base and curing agent is prepared through the spin-coating method. The PDMS is then placed on the coating, and a thin layer of mixed liquid is dipped before bonding with the TiO_2/Au nanocomposite film. Finally, the PDMS and TiO_2/Au nanocomposite film are baked at 70 °C for 2 h to enhance the bonding between them, yielding the LOC test device. The three-dimensional (3D) diagram of the fabricated LOC device is shown in Figure 4b, and its layered structure is shown

 doi:10.20944/preprints202401.1637.v1

in Figure 5. The device consists of four parts: a quartz substrate at the bottom, PDMS with microfluidic channels at the top, and a metal-doped and photocatalyst layer in the middle.

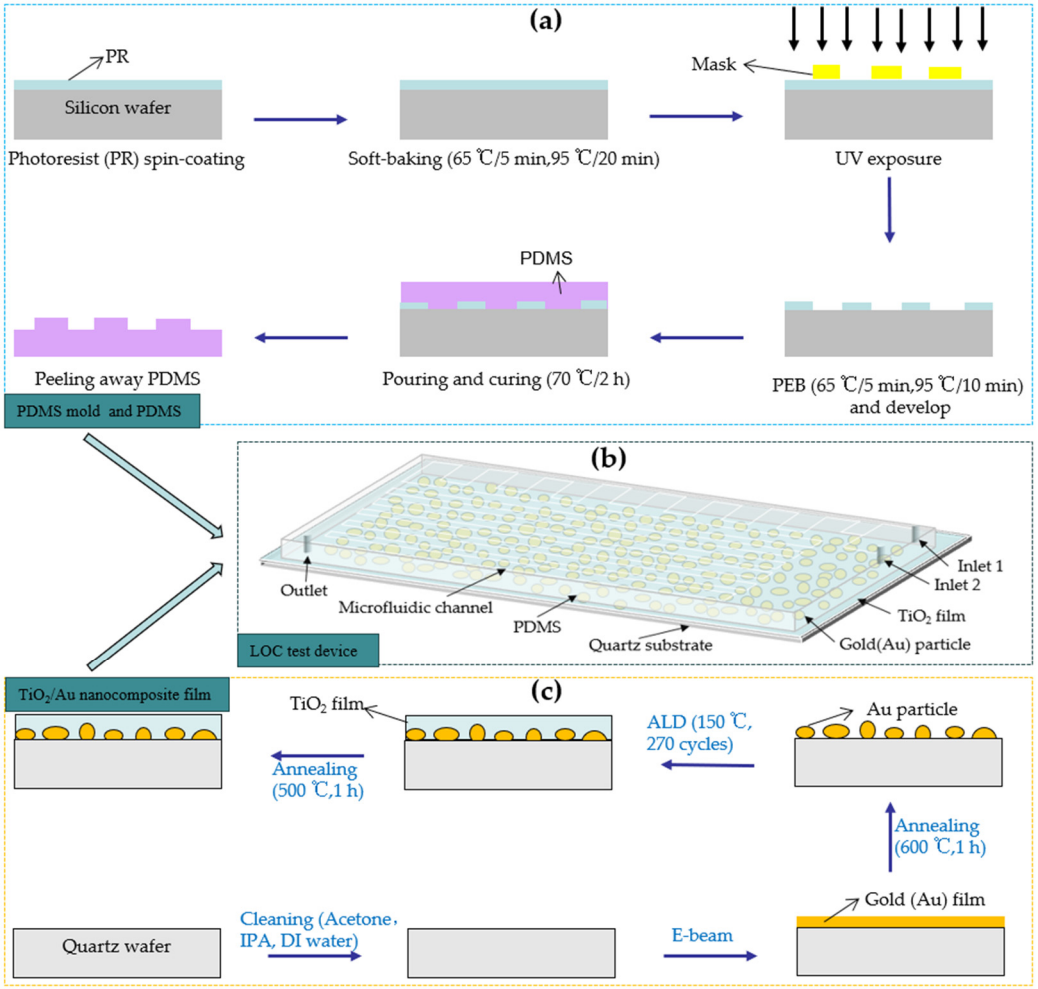

Figure 4. (a) Fabrication process of PDMS mold and PDMS, **(b)** 3D diagram of LOC test device and **(c)** the fabrication process of TiO_2/Au nanocomposite film on a quartz substrate.

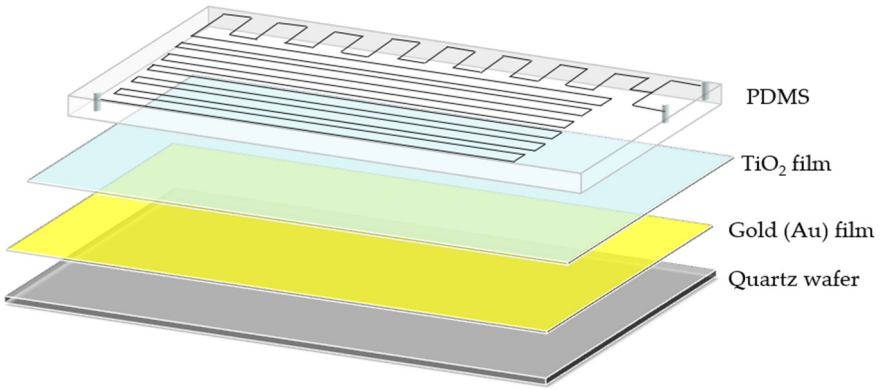

Figure 5. 3D layered structure diagram of LOC device.

2.4. Performance Evaluation of TiO_2/Au Nanocomposite Film

RhB, an organic compound dye (typically red in color), is often used with methyl blue or methyl orange dyes for the photocatalytic degradation of pollutants [25–27]. In this study, RhB is selected as the test sample for photocatalytic degradation experiments to verify the performance of TiO_2/Au

 doi:10.20944/preprints202401.1637.v1

nanocomposite film. All the chemicals were purchased from Duksan Pure Chemicals Co., Ltd. (Ansan city, Korea)

During the experiment, RhB and $K_2S_2O_8$ are connected by a hose on the micropump, facilitating uniformly flow from the input port into the microchannel for photocatalytic reaction. The micropump flow rates are 59.38, 27.19, 17.76, 13.87, 11.10, and 8.88 uL/min, corresponding to photocatalytic reaction durations of 1, 2, 3, 4, 5, and 6 min, respectively. The photocatalytic degradation efficiency of TiO_2/Au nanocomposite film with different thicknesses of gold film and pure TiO_2 is measured by adjusting the micropump flowrate to vary the photocatalytic reaction duration. The inner diameter of the hose connecting the input to the test sample is 0.25 mm. The absorbance of the photocatalytic degradation solution, collected in a petri dish at the outlet, is measured using a UV–vis spectrophotometer (AOE UV-1800PC, Shanghai, China) and compared with the original concentration. In all experiments, UV light with a wavelength of 365 nm and power of 5 W is irradiated from the back.

2.5. TP Experiment by LOC Device and Autoclave

Before initiating the TP experiment, it is necessary to identify the relationship between different concentrations of PO_4^{3-} solutions and their absorbance after staining using standard solutions (potassium phosphate monobasic, KH_2PO_4). Thus, pre-prepared PO_4^{3-} solutions with different concentrations (0.0, 0.1, 0.5, 1, and 2 mg/1000 mL) are mixed with the coloring agent. The mixed liquid initially appears blue, and the color gradually darkens as the PO_4^{3-} concentration increases. The relationship between the PO_4^{3-} concentration and absorbance is determined using a UV–vis spectrophotometer to measure the absorbance of the blue mixture.

The relationship between PO_4^{3-} concentration and absorbance is determined using a standard solution. Therefore, in the following TP experiment, sodium glycerophosphate ($C_3H_7Na_2O_6P$) is selected as the original phosphorus solution. To assess the pretreatment effect of phosphorus-containing compounds under different photocatalytic reaction durations, phosphorus-containing compounds with a concentration of 1 mg/1000 mL are selected as analytes. The concentration of $K_2S_2O_8$ (oxidizing agent) is 8 g/1000 mL. The prepared phosphorus-containing solution and oxidizing agent are added into a vial in a 1:1 ratio (total volume of 20 mL) and placed into the reaction chamber of the autoclave for 30 min to undergo pretreatment at a high temperature (121 °C) and high pressure (1.1 kg/cm^2).

The other analyte is pretreated using the LOC device with a 2-nm gold film through photocatalysis. The phosphorous solution and oxidizing agent are fed to the microchannel through micropump hoses, and the mixture after the photocatalytic reaction is collected in a petri dish at the output. The micropump flow rates are 11.10, 4.995, 3.885, 2.775, 2.220, and 1.665 μL/min, corresponding to photocatalytic reaction durations of 5, 10, 15, 20, 25, and 30 min, respectively. Throughout the experiments, UV light with a wavelength of 365 nm and power of 5 W is irradiated from the back. The inner diameter of the hose connecting the input to the test sample is 0.25 mm.

According to the results of these photocatalytic degradation experiments with different photocatalytic reaction durations and a comparison with the autoclave results, the LOC device and autoclave yield similar pretreatment effects when the photocatalytic time is 15 min. Finally, solutions containing phosphorus compounds with concentrations of 0 mg/1000 mL to 1 mg/1000 mL are photocatalyzed for 15 min, and the absorbance value obtained after dyeing is compared with that obtained by the autoclave.

The PO_4^{3-} concentration in the experiment is distinguished using a colorant composed of ammonium molybdate ($(NH_4)_6Mo_7O_{24}{\cdot}4H_2O$), potassium antimony tartrate ($KSbC_4H_4O_7{\cdot}1/2H_2O$), ascorbic acid ($C_6H_8O_6$), and sulfuric acid ($H_2SO_4$). The prepared colorant and PO_4^{3-}-containing reagent are mixed in a 1:1 (vol.) ratio, and the absorbance of the sample is measured by UV–vis spectrophotometry after standing for 15 min. The observed color depth varies with the PO_4^{3-} concentration.

 doi:10.20944/preprints202401.1637.v1

3. Results and Discussion

3.1. Characterization of Materials

Figure 6 shows images of gold film before annealing, heat-treated gold films, and TiO_2/Au nanocomposite film on a quartz substrate, captured by scanning electron microscopy (SEM; Hitachi S-4800, Tokyo, Japan). Figures 6a–d indicate that the gold nanoparticles exhibit irregular island-like structures and are evenly distributed on the quartz substrate. After heat treatment (600 ℃, 1 h), the shape of the gold nanoparticles changes to nearly spherical. The average size of the gold nanoparticles increases with the increase in the gold film thickness (Figures 6e–h), primarily due to the enhanced aggregation effect of gold nanoparticles during heat treatment [28,29]. The SEM images of the TiO_2/Au nanocomposite film (Figures 6i–l) show that the deposited TiO_2 film forms a conformal pinhole-free layer, and heat treatment does not affect the size and distribution of gold nanoparticles.

Figure 7 shows the X-ray diffraction (XRD; Bruker D8 Discover, Karlsruhe, Germany) patterns of the annealed TiO_2 and TiO_2/Au nanocomposite films. Figure 7a indicates that pure TiO_2 annealed at high temperature (500 ℃, 1 h) presents an anatase phase with high photocatalytic activity [30,31]. The peaks of the diffraction patterns appear at 2θ = 25.24°, 38.24°, 49.52°, 53.92°, and 64.16°, corresponding to the (101), (004), (200), (105), and (116) anatase structure planes, respectively (JCPDS file no.21-1271).

Moreover, despite being doped with gold films of varying thicknesses, the TiO_2 in the doped TiO_2/Au nanocomposite film exhibits an anatase structure with high photocatalytic activity (Figures 7b–e). The crystal structure of TiO_2 is not affected by the deposition of gold films with different thicknesses. For the TiO_2/Au nanocomposite film with a thickness of 2 nm, diffraction peaks of Au crystal planes appear at 2θ = 38.12°, 44.44°, and 64.16° (JCPDS file no. 04-0784). Other TiO_2/Au nanocomposite film also exhibit similar diffraction peaks at these 2θ angles because the difference in the thickness of the deposited gold film leads to variations in the diffraction peak height is different. The specific trend is that the diffraction peak of the gold film increases with the increase in the deposition thickness [32,33].

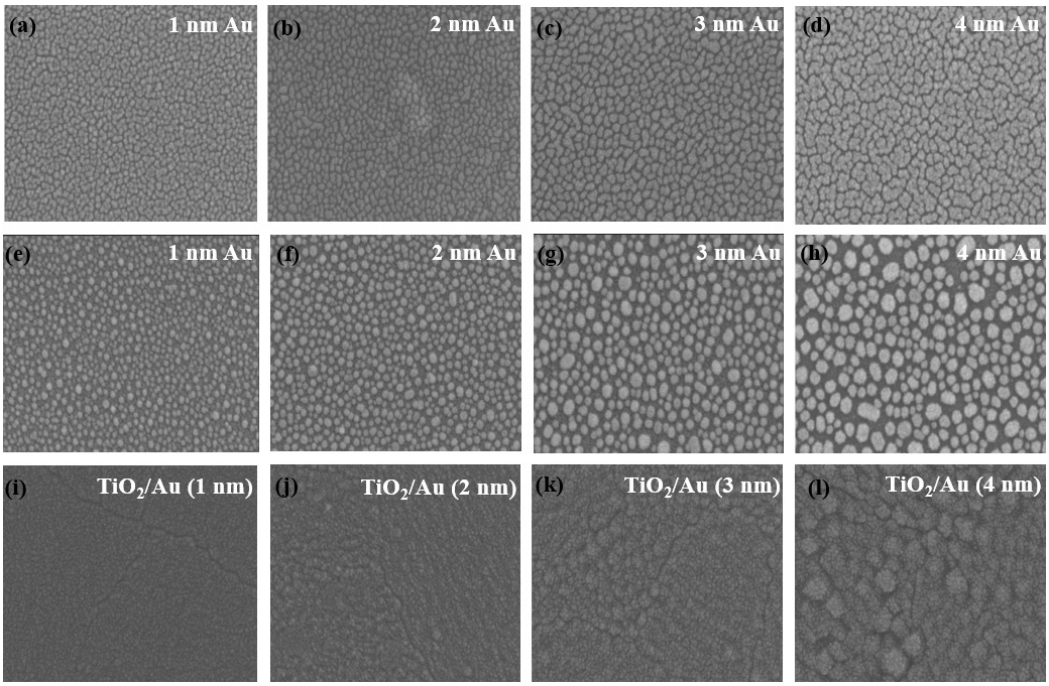

Figure 6. SEM images of gold film before annealing **(a, b, c, d)** and gold film **(e, f, g, h)** and TiO_2/Au nanocomposite film **(i, j, k, l)** after annealing. (Au: 600 ℃, 1 h. TiO_2/Au: 500 ℃, 1 h).

 doi:10.20944/preprints202401.1637.v1

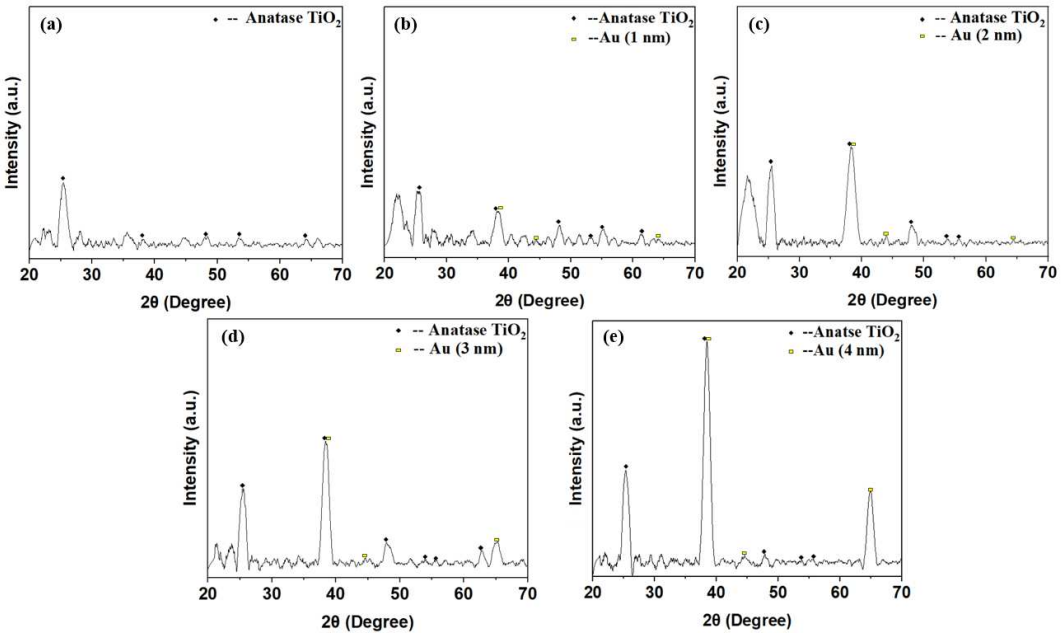

Figure 7. XRD patterns of pure TiO_2 and TiO_2/Au nanocomposite films after annealing.

3.2. Photocatalytic Degradation Performance

Figure 8a shows the absorbance of RhB by the LOC device with different gold films deposition thicknesses for a photocatalytic reaction time of 1 min. The peak absorbance after photocatalytic degradation is 550 nm. Thus, comparing the peak values at 550 nm, the photocatalytic degradation performance of different LOC detection devices can be discerned.

The experimental results (Figure 8b) show that the deposition of gold films enhances the photocatalytic degradation efficiency compared with that attained using pure TiO_2. When the photocatalytic reaction time is 1 min, the performance difference between the various LOC detection devices is the most pronounced. As the photocatalytic reaction time increases, this gap gradually decreases, because each detection device demonstrates almost complete degradation of RhB. When the photocatalytic time is 6 min, RhB is completely degraded, and there is no significant difference in the photocatalytic degradation performances of LOC device with different noble metal film deposition thicknesses. However, regardless of the photocatalytic reaction period, the LOC detection device with a metal film deposition thickness of 2 nm exhibits the highest photocatalytic degradation efficiency. This observation indicates that when the thickness of the gold film is 2 nm, the UV light absorption and interface of the TiO_2 and gold nanoparticles are optimized, and the highest photocatalytic degradation performance can be achieved. When the thickness of the deposited gold film is greater than 2 nm, the photocatalytic activity of TiO_2/Au nanocomposite film deteriorates, attributable to the aggregation of gold nanoparticles in excessively thick gold films, which hinders effective light absorption on the TiO_2/Au nanocomposite film. The transmittance test results of TiO_2/Au nanocomposite film (Figure 9) confirm these observations.

Figure 10a shows the absorbance of a standard solution with different PO_4^{3-} concentrations (0.0, 0.1, 0.5, 1, 2 mg/1000 mL) after coloring. With increase in the PO_4^{3-} concentration, the absorbance gradually increases, verifying the positive correlation between the PO_4^{3-} concentration and absorbance. Figure 10b, showing the images of different PO_4^{3-} solution concentrations after coloring, further confirms the absorbance test results discussed above. Moreover, the peak absorbance of the PO_4^{3-} solution after coloring is mainly 880 nm, and the concentration of the PO_4^{3-} solution can thus be determined by comparing the absorbance value at 880 nm.

 doi:10.20944/preprints202401.1637.v1

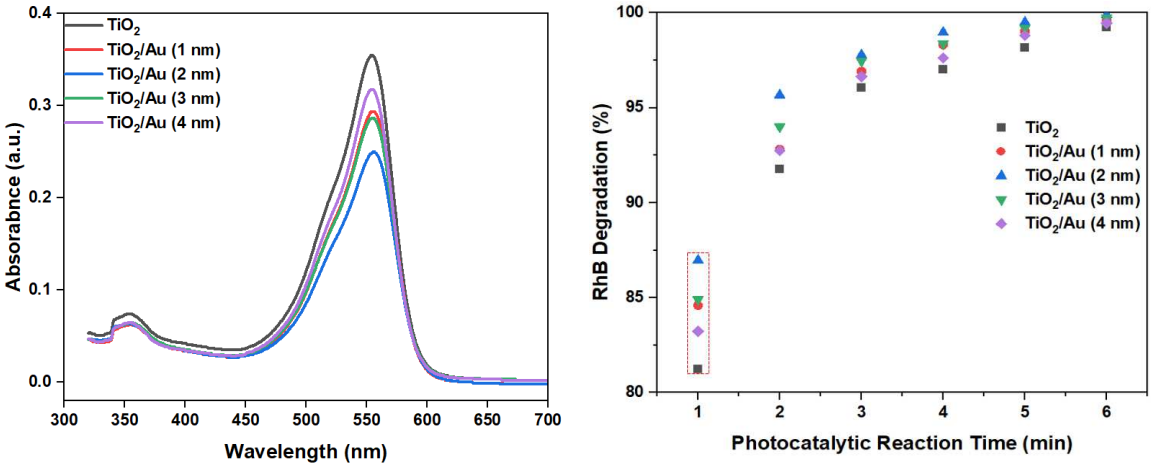

(a) (b)

Figure 8. (a) Absorbance of RhB when the photocatalytic reaction time is 1 min, and **(b)** RhB degradation graph at 550 nm with different LOC devices under different photocatalytic reaction durations.

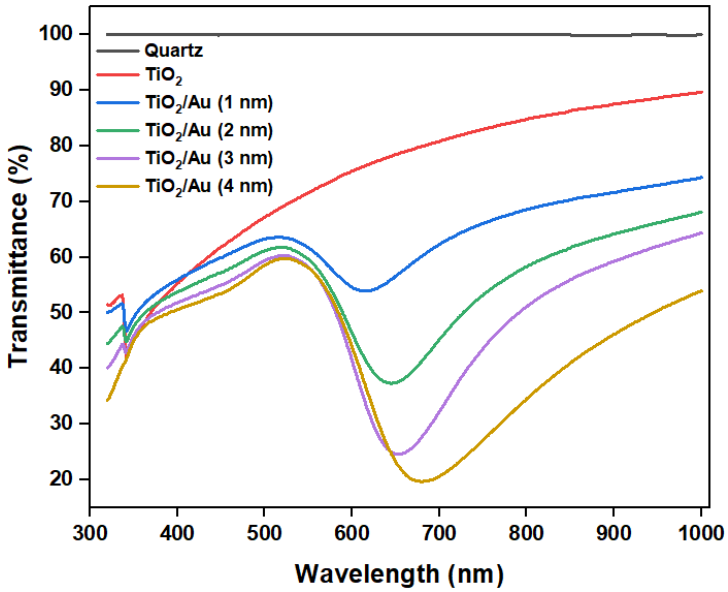

Figure 9. Transmittance of TiO_2 and TiO_2/Au nanocomposite films with different deposition thicknesses of gold films.

Overall, the photocatalytic degradation experiment results of RhB indicate that when the deposition thickness of the noble metal film is 2 nm, the TiO_2/Au nanocomposite film exhibits the highest photocatalytic degradation efficiency. Moreover, the absorbance test of PO_4^{3-} standard solution with different concentrations verifies the positive correlation between the PO_4^{3-} concentration and absorbance.

 doi:10.20944/preprints202401.1637.v1

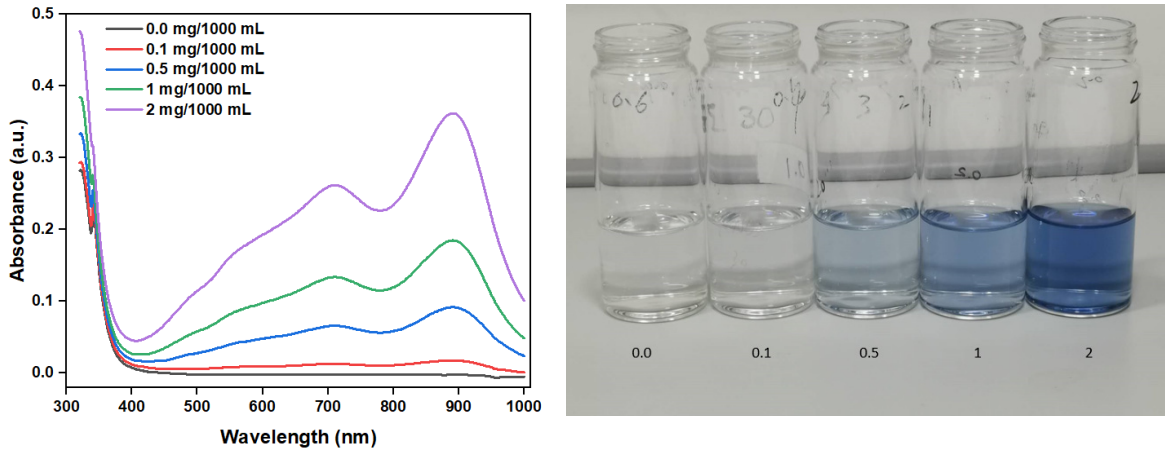

(**a**) (**b**)

Figure 10. (a) Measured absorbance of standard solution with different concentrations of phosphate and **(b)** images of solutions with different phosphate concentrations after coloring.

Figure 11a shows the absorbance of the photocatalytic degradation of a phosphorous-containing solution with a TP concentration of 1 mg/1000 mL under different photocatalytic reaction durations, using an LOC device with a gold film deposition thickness of 2 nm and an autoclave. The peak absorbance at 880 nm is shown in Figure 11b. The absorbance increases with the increase in the photocatalytic reaction time. This observation indicates that with the increase in the photocatalytic reaction time, more phosphorus-containing compounds decompose into PO_4^{3-}. However, when the photocatalytic time is greater than 25 min, the absorbance is saturated. This finding suggests that at 25 min, phosphorous-containing compounds with a concentration of 1 mg/1000 mL are completely decomposed, and further prolonging the photocatalytic reaction time does not increase the PO_4^{3-} concentration.

From the absorbance test results of phosphorus-containing compound solutions with a TP concentration of 1 mg/1000 mL under different photocatalytic reaction durations, we can conclude that the LOC test device with a gold film deposition thickness of 2 nm can achieve a pretreatment performance similar to that of the autoclave when the photocatalytic reaction time is 15 min. Therefore, an LOC test device with a gold film deposition thickness of 2 nm is used to pretreat a phosphorous compound with concentrations ranging from 0 mg/1000 mL to 1 mg/1000 mL for a photocatalytic reaction duration of 15 min, and the results are compared with those obtained using an autoclave. The experimental results (Figure 12) show that when the duration is 15 min, the LOC device with a deposition thickness of 2 nm can obtain a pretreatment effect similar to that of the autoclave. The measured absorbance with variations in phosphorus concentration using the LOC test device with a gold film thickness of 2 nm exhibits similar trends as that of the conventional equipment (autoclave). In general, the variations in concentration and absorbance corresponding to the LOC device and autoclave can be expressed by the following equations:

$$\text{Autoclave: } y(\text{Absorbance}) = 0.18427x\ (\text{TP Concentration}) + 0.00318 \quad (5)$$

$$\text{LOC Device: } y(\text{Absorbance}) = 0.18384x\ (\text{TP Concentration}) + 0.00391 \quad (6)$$

Thus, the phosphorus concentration of an unknown analyte can be calculated using the LOC device, based on the provided equation relating the phosphorus concentration and absorbance.

The results from the two different TP pretreatment experiments show that the LOC detection device is a promising substitute to the traditional autoclave equipment, effectively addressing the limitations high cost, large volume, and prolonged response time associated with traditional equipment. Compared with traditional autoclaves, the LOC device is cost-effective and compact, in line with the increasing demand for on-site testing.

 doi:10.20944/preprints202401.1637.v1

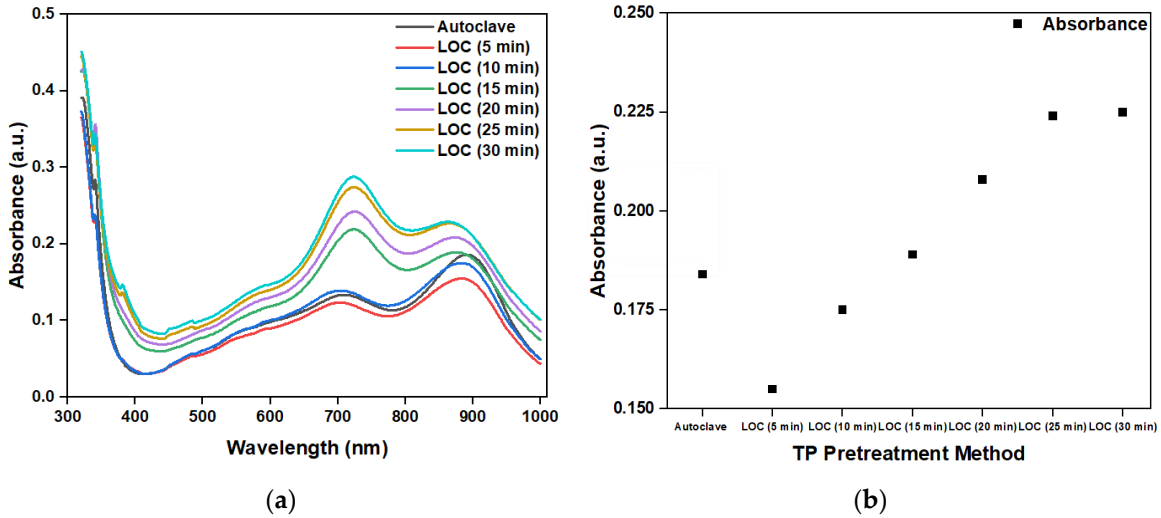

(a) (b)

Figure 11. (a) Measured absorbance of phosphorus-containing analyte using the autoclave and LOC device under different photocatalytic reaction durations and **(b)** peak values at 880 nm.

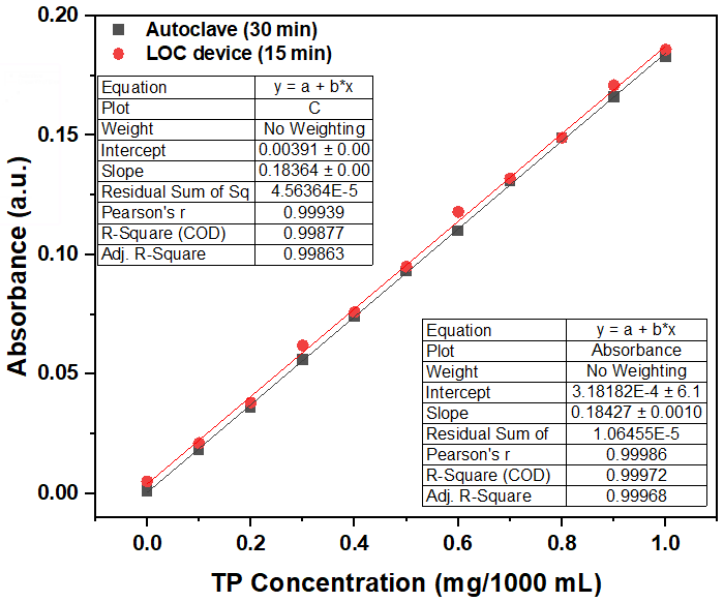

Figure 12. Comparative results of LOC device and autoclave, used to determine the relationship between the TP concentrations and absorbance. (wavelength = 880 nm; photocatalytic reaction time of 15 min).

5. Conclusions

This paper introduces a TiO_2/Au deposition method to address challenges related to gold film detachment and oxidation of gold particles during experiments. The Schottky barrier formed by the direct connection of metal nanoparticles and TiO_2 film helps inhibit the recombination of electron–hole pairs [11,15,34]. The use of back irradiation increases the utilization rate of incident light and avoids the potential obstruction effects of PDMS, TP, or RhB reagents on incident light.

Subsequently, different heat-treatment temperatures are applied to the deposited gold film and TiO_2 film to minimize the influence of TiO_2 heat treatment on the size and distribution of gold nanoparticles. Lastly, the photocatalytic degradation performance of TiO_2 and its enhancement by gold-film doping are verified using RhB dye and $K_2S_2O_8$ oxidizing agent. A comparative analysis reveals that the photocatalytic performance of TiO_2 is enhanced the most when the doping thickness of gold films is 2 nm. Further increase in the deposition thickness of the gold film deteriorates the photocatalytic efficiency owing to reduced direct contact surface between the gold particles and TiO_2,

which reduces the reaction rate. Moreover, multilayer stacking reduces the light absorption and utilization [35,36].

An LOC test device with a deposition thickness of 2 nm and an autoclave are used to pretreat phosphorus-containing compounds with identical concentrations. The photocatalytic time is modified by adjusting the flow rate of the micropump, and the absorbance of the pretreated sample under different photocatalytic durations is compared with that of the sample pretreated by the conventional method (autoclave). The results indicate that when the photocatalytic reaction time is 15 min, the TP pretreatment with LOC device achieves nearly identical pretreatment performance as the traditional autoclave method. Finally, the results obtained by the LOC device (reaction time: 15 min) for pretreating phosphorus-containing solutions with concentrations ranging from 0 mg/1000 mL to 1 mg/1000 mL are compared with those of the autoclave. The experimental results further verify the feasibility of the LOC equipment replacing traditional autoclave equipment.

Notably, although noble metal deposition can enhance the photocatalytic performance of TiO_2, various factors such as the preparation method, film deposition thickness, crystal structure, and the size and shape of noble metal particles also significantly influence the photocatalytic degradation performance of TiO_2 and must be considered.

Author Contributions: Conceptualization, J.J.W., and S.D.K.; Formal analysis, J.Y.L., J.S.K.; Investigation, J.J.W.; Supervision, S.D.K., M.H. and S.H.K.; LOC device fabrication, N.J., and H.K.; Writing-Review and editing, J.J.W., S.H.K.; Sample analysis, D.Y.K., and Y.N. All authors have read and agreed to the published version of the manuscript.

Funding: This research was supported by The Korea Innovation Foundation (INNOPOLIS) grant funded by the Korea government (MSIT) (2020-DD-UP-0348), and Ministry of Environment as "The Eco-technopia 21 projects" (RS-2023-00218010), and the BK21 FOUR project funded by the Ministry of Education, Korea (4199990113966).

Institutional Review Board Statement: Not applicable

Informed Consent Statement: Not applicable

Data Availability Statement: Data are contained within the article.

Conflicts of Interest: The authors declare no conflict of interest.

References

1. Shen, J.; Yuan, L.; Zhang, J.; Li, H.; Bai, Z.; Chen, X.; Zhang, W.; Zhang, F. Phosphorus Dynamics: From Soil to Plant. Plant Physiology, 2011, 156, 997-1005.
2. Conley, D.J.; Paerl, H.W.; Howarth, R.W.; Boesch, D.F.; Seitzinger, S.P.; Havens, K.E.; Lancelot, C.; Likens, G.E. Controlling Eutrophication: Nitrogen and Phosphorus. Science, 2009, 323, 1014-1015.
3. Xiao, X.; Agustí, S.; Pan, Y.; Yu, Y.; Li, K.; Wu, J.; Duarte, C.M. Warming Amplifies the Frequency of Harmful Algal Blooms with Eutrophication in Chinese Coastal Waters. Environ. Sci. Technol, 2019, 53, 13031-13041.
4. Le, C.; Zha, Y.; Li, Y.; Sun. D.; Lu, H.; Yin, B. Eutrophication of Lake Waters in China: Cost, Causes, and Control. Environmental Management, 2010, 45, 662-668.
5. O'Neil, J.M.; Davis, T.W.; Burford, M.A.; Gobler, C.J. The rise of harmful cyanobacteria blooms: The potential roles of eutrophication and climate change. Harmful Algae, 2012, 14, 313-334.
6. Nakata, K.; Fujishima, A. TiO_2 photocatalysis: Design and applications. Journal of Photochemistry and Photobiology C: Photochemistry Reviews. 2012, 13, 169-189.
7. Wang, N.; Lei, L.; Zhang, X.M.; Tsang, Y.H.; Chen, Y.; Chan, Helen L.W. A comparative study of preparation methods of nanoporous TiO_2 films for microfluidic. Microelectronic Engineering, 2011, 88, 2797-2799.
8. Kusiak-Nejman, E.; Morawski, A.W. TiO_2/graphene-based nanocomposites for water treatment: A brief overview of charge carrier transfer, antimicrobial and photocatalytic performance. Applied Catalysis B: Environmental, 2019, 253, 179-186.
9. Birnal, P.; Marco de Lucas, M.C.; Pochard, I.; Herbst, F.; Heintz, O.; Saviot, L.; Domenichini, B.; Imhoff, L. Visible-light photocatalytic degradation of dyes by TiO_2-Au inverse opal films synthesized by Atomic Layer Deposition. Applied Surface Science, 2023, 609, 155213.
10. Armelao, L.; Barreca, D.; Bottaro, G.; Gasparotto, A.; Maccato, C.; Maragno, C.; Tondello, E.; Štangar, U.L.; Bergant, M.; Mahne, D. Photocatalytic and antibacterial activity of TiO_2 and Au/TiO_2 nanosystems. Nanotechnology, 2007, 18, 375709.

11. Lin, L.; Zhong, Q.; Zheng, Y.; Cheng, Y.; Qi, R.; Huang, R. Size effect of Au nanoparticles in Au-TiO_{2-x} photocatalyst. Chemical Physics Letters, 2021, 770, 138457.
12. Jung, D.G.; Jung, D.; Kong, S.H. Characterization of Total-Phosphorus (TP) Pretreatment Microfluidic Chip Based on a Thermally Enhanced Photocatalyst for Portable Analysis of Eutrophication. sensor, 2019, 19, 3452.
13. Jung, D.G.; Jung, D.; Kong, S.H. Lab-on-a-chip based total-phosphorus analysis device utilizing a photocatalytic rection. Solid-State Electronics, 2018, 140, 100-108.
14. Jung, D.G.; Han, M.; Kim, S.D.; Kwon, S.Y.; Kwon, J.; Lee, J.; Kong, S.H.; Jung, D. Miniaturized Portable Total Phosphorus Analysis Device Based on Photocatalytic Reaction for the Prevention of Eutrophication. Micromachines, 2019, 12, 1062.
15. Linsebigler, A.L.; Lu, G.; Yates, J.Y.; Jr. Photocatalysis on TiO2 surfaces: Principles, Mechanisms, and Selected Result. Chem. Rev. 1995, 95, 735-758.
16. Parka, H.; Park, Y.; Kimb, W.; Choi, W. Surface modification of TiO_2 photocatalyst for environmental applications. Journal of Photochemistry and Photobiology C: Photochemistry Reviews, 2013, 15, 1-20.
17. Chen, D.; Cheng, Y.; Zhou, N.; Chen, P; Wang, Y.; Li, K.; Huo, S.; Cheng, P.; Peng, P.; Zhang, R.; Wang, L.; Liu, H.; Liu, Y.; Ruan, R. Photocatalytic degradation of organic pollutants using TiO_2-based photocatalysts: A review. Journal of Cleaner Production, 2020, 268, 121725.
18. Parrino, F.; Livraghi, S.; Giamello, E.; Ceccato, R.; Palmisano, L. Role of Hydroxyl, Superoxide, and Nitrate Radicals on the Fate of Bromide Ions in Photocatalytic TiO_2 Suspensions. ACS Catalysis, 2020, 10, 7922-7931.
19. Yang, L.M.; Yu, L.E.; Ray, M.B. Photocatalytic Oxidation of Paracetamol: Dominant Reactants, Intermediates, and Reaction Mechanisms. Environmental Science & Technology, 2009, 43, 460-465.
20. Kawasaki, M.; Chen, M.; Yang, J.; Chiou, W.; Shiojiri, M. Structural analysis of Au/TiO_2 thin films deposited on the glass substrate. Applied Physics Letters, 2013, 102, 091603.
21. Reiners, M.; Xu, K.; Aslam, N.; Devi, A.; Waser, R.; Hoffmann-Eifert, S. Growth and Crystallization of TiO_2 Thin Films by Atomic Layer Deposition Using a Novel Amido Guanidinate Titanium Source and Tetrakis-dimethylamido-titanium. Chemical of Materials, 2013, 25, 2934-2943.
22. Byrne, C.; Fagan, R.; Hinder, S.; McCormack, D.E.; Pillai, S.C. New approach of modifying the anatase to rutile transition temperature in TiO_2 photocatalysts RCS Advances, 2016, 6, 95232-95238.
23. Mathpal, M.C.; Tripathi, A.K.; Singh, M.K.; Gairola, S.P.; Pandey, S.N.; Agarwal, A. Effect of annealing temperature on Raman spectra of TiO_2 nanoparticles. Chemical physics Letters, 2013, 555, 182-186.
24. Lu, Y.; Chen, S.; Quan, X.; Yu, H.; Fabrication of a TiO_2/Au Nanorod Array for Enhanced Photocatalysis. Chinese Journal of Catalysis, 2011, 32, 1838-1843.
25. Zhuang, J.; Dai, W.; Tian, Q.; Li, Z.; Xie, L.; Wang, J.; Liu, P.; Shi, X.; Wang, D. Photocatalytic Degradation of RhB over TiO_2 Bilayer Films: Effect of Defects and Their Location. Langmuir, 2010, 26, 9686-9694.
26. Rizzo, L.; Koch, J.; Belgiorno, V.; Anderson, M.A.; Removal of methylene blue in a photocatalytic reactor using polymethylmethacrylate supported TiO_2 nanofilm. Desalination, 2007, 211, 1-9.
27. Wang. X.; Hu, Z.; Chen, Y.; Zhao, G.; Liu, Y.; Wen, Z. A novel approach towards high-performance composite photocatalyst of TiO_2 deposited on activated carbon. Applied Surface Science, 2009, 255, 3953-3958.
28. Alizadeh, S.; Nazari, Z. A Review on Gold Nanoparticles Aggregation and Its Application. Chemical Reviews, 2020, 2, 228-242.
29. LeGore, L.J.; Lad, R.J.; Vetelino, J.F.; Frederick, B.G.; Kenik, E.A. Aggregation and sticking probability of gold on tungsten trioxide films. Sensors and Actuators B: Chemical, 2001, 76, 373-379.
30. Lin, C.P.; Chen, H.; Nakaruk, A.; Koshy, P.; Sorrell, C.C. Effect of Annealing Temperature on the Photocatalytic Activity of TiO_2 Thin Films. Energy Procedia, 2013, 34, 627-636.
31. Sankapal, B.R.; Lux-Steiner, M. Ch.; Ennaoui, A. Synthesis and characterization of anatase-TiO_2 thin films. Applied Surface Science, 2005, 239, 165-170.
32. Kim, D. Influence of Au thickness on the optical and electrical properties of transparent and conducting TiO_2/Au multilayer films. Optical Communications, 2010, 283, 1792-1794.
33. Sriubas, M.; Kavaliunas, V.; Bockute, K.; Palevicius, P.; Kaminskas, M.; Rinkevicius, Z.; Ragulskis, M.; Laukaitis, G. Formation of Au nanostructure on the surface of annealed TiO_2 thin film. Surface and Interfaces, 2021, 25, 101239.
34. Sakthivel, S.; Shankar, M.V.; Palanichamy, M.; Arabindoo, B.; Bahnemann, D.W.; Murugesan, V. Enhancement of photocatalytic activity by metal deposition: characterization and photonic efficiency of Pt, Au and Pd deposited on TiO_2 catalyst. Water research,2004, 38, 3001-3008.

 doi:10.20944/preprints202401.1637.v1

35. Arabatzis, I.M.; Stergiopoulos, T.; Andreeva, D.; kitova, S.; Neophytides, S.G.; Falaras, P. Characterization and photocatalytic activity of Au/TiO_2 thin films for azo-dye degradation. Journal of Catalysis, 2003, 220, 127-135.
36. Wu, Y.; Liu, H.; Zhang, J.; Chen, F.; Enhanced Photocatalytic Activity of Nitrogen-Doped Titania by Deposited with Gold. The Journal of physical Chemistry C, 2009, 113, 14689-14695.